Journal of Power Sources 184 (2008) 331–335

Contents lists available at ScienceDirect

Journal of Power Sources

journal homepage: www.elsevier.com/locate/jpowsour

Short communication

Columnar rutile TiO_2 based dye-sensitized solar cells by radio-frequency magnetron sputtering

Soon Hyung Kang[a], Moon-Sung Kang[b], Hyun-Sik Kim[a], Jae-Yup Kim[a], Young-Hoon Chung[a], William H. Smyrl[c], Yung-Eun Sung[a,*]

[a] School of Chemical and Biological Engineering and Interdisciplinary Program in Nano Science and Technology, Seoul National University, Seoul 151-742, South Korea
[b] Energy and Environmental Laboratory, Samsung Advanced Institute of Technology, Gyeonggi-Do 446-712, South Korea
[c] Corrosion Research Center, Department of Chemical Engineering and Materials Science, University of Minnesota, Minneapolis, MN 55455, USA

ARTICLE INFO

Article history:
Received 4 April 2008
Received in revised form 6 May 2008
Accepted 29 May 2008
Available online 20 June 2008

Keywords:
Rutile TiO_2
Columnar structure
Dye-sensitized solar cell
Radio-frequency magnetron sputtering
Substrate heating
Photocurrent

ABSTRACT

Columnar-structured rutile TiO_2 film with a thickness of 1.4 μm is prepared using the radio-frequency (RF) magnetron sputtering technique, for application in dye-sensitized solar cells (DSSCs). Pure rutile TiO_2 films are fabricated by controlling the substrate temperature during sputtering and using a substrate with a rough surface morphology. Successive substrate heating to 623 K induces the growth of a rutile TiO_2 film that has a specific direction in the (1 1 0) plane, which results in a decrease in the average grain size. This causes in an increase of dye uptake and thereby contributes to enhancement of the photocurrent in the DSSC.

1. Introduction

For the last decade, after a major breakthrough [1], the dye-sensitized solar cell (DSSC) has been extensively investigated in terms of many types of components and interfaces, as a replacement for expensive silicon-based inorganic solar cells. In particular, several aspects of a photoanode layer have been examined, for use with materials such as one-dimensional nano-materials (e.g., nanorods, nanowires, nanotubes) [2–4], different metal oxide materials (e.g., ZnO, SnO_2, Al_2O_3, MgO) [5–7], doped metal oxide materials using a doping source (e.g., N, C, S, P) [8,9], and the evaluation of electron transport/charge recombination in a nanoporous network [10,11]. In addition, the interfacial contact properties between the semiconductor metal oxide layer and the transparent conducting oxide (TCO) have been considered to play a very important role in the enhancement of the photovoltaic performance of DSSCs.

Recently, greater charge-collection efficiency by inserting a self-assembled TiO_2 nanoparticle layer between the mesoporous TiO_2 and TCO has been reported [12]. It was demonstrated that the well-developed thin interlayer provided a superior interfacial contact property with TCO, and therefore enhanced electron lifetime by suppressing charge recombination. Moreover, a nanoporous interlayer structure with a uniform pore size (~10 nm) increased the amount of dye adsorption of the photoelectrode that resulted in enhancement of the photocurrent. Similarly, to reduce the charge recombination at the TCO|TiO_2 interface, several researchers have proposed the use of a blocking layer in the TCO substrate to prevent direct contact with the electrolyte. The layer consists of metal oxides with thin and compact structures, using spray pyrolysis [13], spin coating [14], dip coating [15], and sputtering [16], etc. Given that the growth of a thin film employing vacuum technology, such as sputtering and evaporation, has a variety of advantages, i.e., easy control, a clean process, reproducibility, high adhesion, and large scale-up [17,18], the formation of a thin film on a TCO substrate has a significant effect on both the conversion efficiency and the commercialization of DSSC.

In this work, columnar-structured TiO_2 layers are developed from radio frequency (RF, 13.56 MHz) magnetron sputtering. The feasibility as an intermediate layer for improving the interfacial contact between mesoporous TiO_2 and TCO is examined. In particular, a systematic investigation of the growth and characterization of a TiO_2 film on a rigid F-doped SnO_2 (FTO) substrate was performed. To elaborate, columnar-structured anatase and rutile TiO_2 film directly grown on the FTO glass was prepared, using the RF magnetron sputtering method. During sputtering, the surface

* Corresponding author. Tel.: +82 2 880 1889; fax: +82 2 888 1604.
E-mail address: ysung@snu.ac.kr (Y.-E. Sung).

0378-7753/$ – see front matter © 2008 Elsevier B.V. All rights reserved.
doi:10.1016/j.jpowsour.2008.05.089

morphologies and phase composition were controlled precisely by substrate temperature. A rutile TiO_2 film grown at 623 K exhibited rough morphologies that resulted from preferential growth in a specific (1 1 0) direction. This corresponded to an increase of the specific surface area and the light scattering effect from the intrinsic properties of the material.

2. Experimental

2.1. Preparation of anatase and rutile TiO_2 film

Optically transparent F-doped SnO_2 (FTO, 8 $\Omega\,cm^{-2}$) was used as a substrate for deposition of TiO_2 films. Titanium dioxide films with a thickness of 1.4 μm (deposition time of 4 h) were grown with the RF magnetron sputtering system that used a 2-in. TiO_2 target (99.99%, DASOM RMS) attached to a metallic Cu back plate, which was positioned 14 cm from the substrate holder. The deposition rate of the TiO_2 film was calculated to be approximately 5.8 nm per min. The base pressure in the process chamber was $<6.67 \times 10^{-5}$ Pa from diffusion pumping. The total gas pressure (P_{tot}) during deposition was 1.73 Pa in an Ar (99.999%, pure) atmosphere. Film deposition was performed under the condition of a 333 K titled angle between the substrate surface and the mean direction of the sputtered flux. The substrate was rotated at a constant velocity and the applied RF power was a constant 100 W. The substrate temperature (T_{sub}) was increased from room temperature (RT, 298 K) to 623 K through the use of a halogen heater lamp during deposition. For phase transformation, from the partially amorphous to the pure anatase/rutile phase, a post-thermal treatment was performed at 673 K for 20 min in ambient air.

2.2. Electrode assembly

The TiO_2 film was immersed in absolute ethanol containing a ruthenium-complex (N719) for 12 h of dye adsorption. After rinsing with ethanol and drying in air, the dye-adsorbed TiO_2 electrodes were assembled, using thermal adhesive films (Surlyn®, DuPont, 60 μm thickness), into a Sandwich-type cell with a counter electrode. Then, Pt-coated counter electrodes were prepared by spreading a drop of 10 mM H_2PtCl_6 in 2-propanol on to FTO glass and heating at 673 K for 15 min in ambient air. A drop of electrolyte solution composed of 0.3 M 1-methyl-3-propylimidazolium iodide (MPII), 0.1 M LiI, 0.05 M I_2, 0.5 M *tert*-butyl pyridine (TBP) in methoxypropionitrile (MPN) was introduced into the cell that was then sealed using cover glass. An illuminated area of 0.25 cm^2 was fabricated by masking the front side.

2.3. Photoelectrochemical measurement and characterizations

The photovoltaic characteristics of DSSCs were evaluated using a 500 W xenon lamp (XIL model 05A50KS source units laid on AM 1.5 filter) with a light intensity of 1 sun (100 mW cm^{-2}). The incident photoelectron to current efficiency (IPCE) was measured using a tungsten lamp with the intensity of approximately 1 mW cm^{-2}. The electron diffusion coefficient (D) and the lifetime (τ) were determined by stepped light-induced transient measurements of photocurrent and voltage (SLIM-PCV), induced by a stepwise change in the laser diode (λ = 635 nm) intensity. The step-down was a small fraction of the laser intensity (approximately 20% of the initial intensity), and it was controlled by a function generator. The photocurrent and voltage transients were monitored using a digital oscilloscope through an amplifier. The D value was estimated from a time constant (τ_c) and the TiO_2 film thickness (ω) using the equation:

$$D = \frac{\omega^2}{2.77\tau_c} \quad (1)$$

The τ value was derived by fitting an exponential function of the photovoltage transient to $\exp(-t/\tau_c)$ [19,20]. The surface and cross-sectional microstructures of the samples were characterized by field-emission scanning electron microscopy (FE-SEM, JEOL Inc.) at 10 kV and 20 mA. The crystallinity of the films was confirmed by high-power X-ray diffraction (XRD, Rigaku D/MAX 2500 V diffractor) with Cu Kα radiation of 40 kV and 100 mA.

3. Results and discussion

Fig. 1 shows the morphological images of pure anatase and rutile TiO_2 film sputtered on the 297 K and 623 K substrate, respectively. Both structures can be formed with sputtering, utilizing the titled position between the gun and the sample holder, a high working pressure for the growth of a thin film, and substrate heating. Under high working pressure, particles impinging on the substrate are in a less energetic state that results from multiple collisions. Thus, it is easy to induce complete and partial amorphous phases, which depend on substrate heating and can be transformed into the highly crystalline anatase and rutile phase after post-thermal treatment [21]. The TiO_2 film sputtered on the unheated substrate exhibits the pure anatase crystalline phase, while pure rutile TiO_2 film is grown on the heated substrate, which provides the additional thermal energy for less energetic particles to find the appropriate lattice sites from the migration [22]. This is correlated with the stability of the phase, which is dependent on the temperature [23]. The implication is that the preferentially formed rutile TiO_2 phase, which is stable at high temperature, is grown with sufficient energy (kinetic energy + thermal energy) to exhibit rough surface morphology in the (1 1 0) plane. By contrast, the anatase phase is preferentially formed at low temperature. In addition, the significant factor for the formation of columnar-structured TiO_2 film is the roughness of the chosen substrate. A rough substrate, with its roughness estimated at approximately a 100 nm scale, plays an essential role in the growth of a columnar structured TiO_2 film. The required condition is that the kinetic energy of atoms or molecules is significantly reduced due to frequent collisions under the high working pressure, so that deposition occurs preferentially on the projected parts due to the short distance between the sample holder and gun. Accordingly, a columnar structure with an axis of projected parts, under constant rotation, can be effectively formed.

Moreover, from XRD spectra (insets) of Fig. 1, the average grain size of the rutile TiO_2 film calculated by Scherrer's equation is approximately 14.1 nm, i.e., four times smaller than that of the anatase TiO_2 film (*i.e.* 53.3 nm). During the process of chemical synthesis, the formation of a pure rutile TiO_2 film with a grain size of this scale is difficult, compared with that of an anatase TiO_2 film. This is because of directed growth in the (1 1 0) plane and phase instability in the nano-sized domain (<14 nm) that result in an increase in the surface area and an improvement in dye uptake [24]. The amount of dye molecules adsorbed on TiO_2 is evaluated by dye desorption using a 1 M NaOH solution. Using an extinction coefficient (ε) of 3748 $cm^{-1}\,M^{-1}$ at 535 nm (N719 dye) [2], the number of dye molecules adsorbed on the pure anatase and rutile TiO_2 electrode is approximately 2.53×10^{15} and 4.25×10^{15}, respectively. A 70% increase in the dye uptake of rutile TiO_2 film demonstrates that the electrode has a larger surface area than that of the anatase TiO_2 electrode.

Fig. 2 shows the photocurrent–voltage (J–V) characteristics and IPCE values for the cells composed of the columnar-structure TiO_2 electrodes. Under illumination (100 mW cm^{-2}, AM 1.5), the

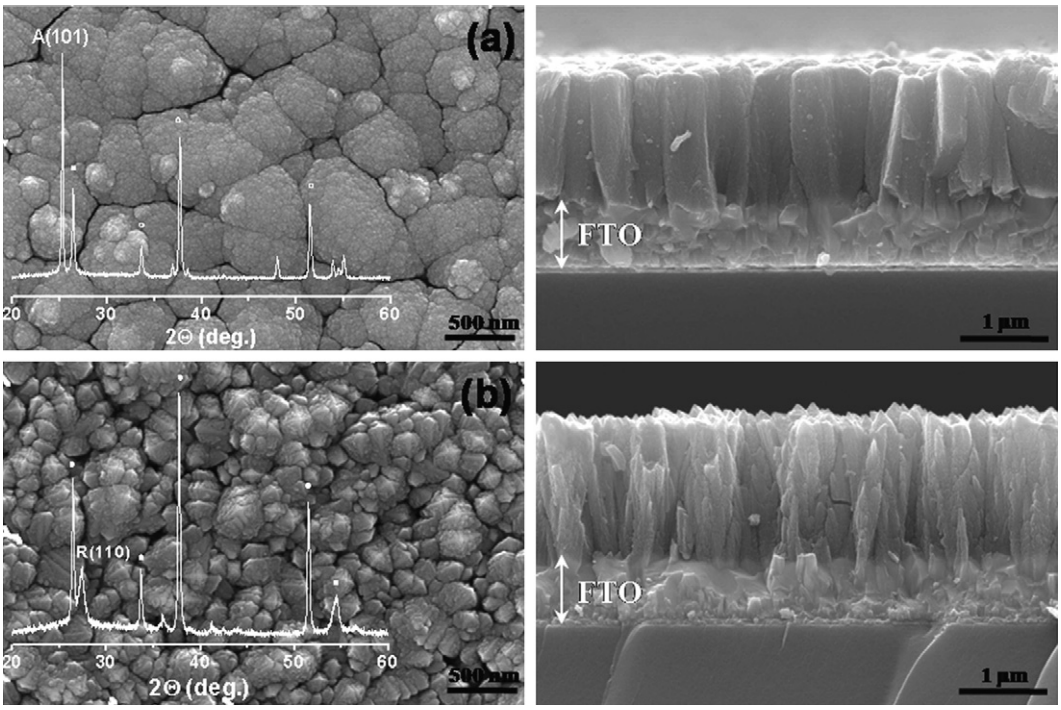

Fig. 1. FE-SEM images of (a) RT sample (pure anatase TiO_2 film) and (b) 623 K sample (rutile TiO_2 film) on FTO substrate. Inset shows XRD spectra of both films (○ indicate peaks of FTO substrate).

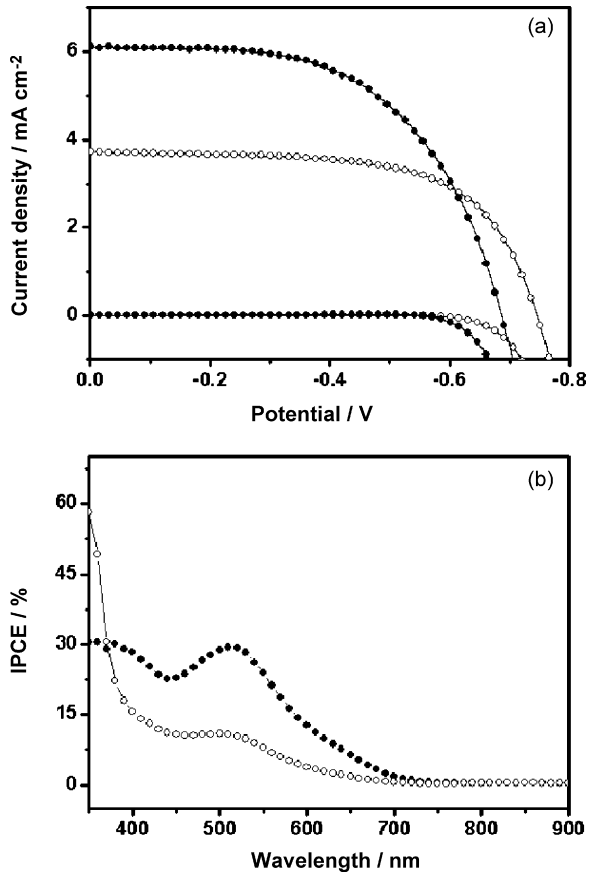

Fig. 2. (a) *J–V* characteristics under illumination and dark states and (b) IPCE spectra as function of wavelength in anatase and rutile TiO_2 photoanode (open circles are anatase TiO_2 film; closed circles are rutile TiO_2 film).

pure rutile TiO_2 photoelectrode exhibits a V_{oc} of 0.687 V, a J_{sc} of 6.12 mA cm^{-2}, a fill factor of 57.1%, and an efficiency of 2.4%, whereas the anatase TiO_2 electrode gives a V_{oc} of 0.745 V, a J_{sc} of 3.71 mA cm^{-2}, a fill factor of 64.2%, and an efficiency of 1.78%. Thus, approximately 35% enhanced conversion efficiency is attained with pure rutile TiO_2 film. Nevertheless, the onset potential of the cell in the dark state is more positive with the rutile TiO_2 electrode by the increase of dark current, coinciding with decreased V_{oc}. This is generally explained to be a result of the increase in charge recombination, predominantly from the photo-injected electrons to the I_3^- ions in the electrolyte, which results from an abrupt increase of photo-injected electrons in the surface region, in the distribution of the limited electron pathways which play a role in the trapping/detrapping sites [25]. Note that a dye uptake of rutile TiO_2, which is approximately twice that of anatase TiO_2, induces both a decrease in the photovoltage and significant increases in the photocurrent.

The IPCE value, which is a function of the wavelength, provides essential information about the morphology and structure of the TiO_2 film. Compared with the anatase TiO_2 electrode, the rutile TiO_2 electrode has a higher IPCE from 400 nm to 750 nm wavelength ranges. The greatly enhanced IPCE at 500–550 nm wavelengths is also attributed to high dye adsorption, which arises from the increased surface area. Furthermore, because it is known that the rutile TiO_2 has a higher refractive index (2.72) than that (2.52) of anatase TiO_2 [26], light scattering, resulting from rough surface morphology at wavelengths of 380–450 nm, can lead to enhancement of the photocurrent. This result will be confirmed further in the next section.

In addition, the ultraviolet–visible (UV–vis) spectroscopy was measured. The UV–vis spectra of bare anatase and the rutile TiO_2 film are presented in Fig. 3. The rutile TiO_2 film exhibits high absorbance across the wavelengths of the entire visible range, in particular a remarkably increased absorbance at wavelengths of 400–500 nm. The inset in Fig. 3 indicates that the band gap of sputtered grown anatase and the rutile TiO_2 film is approximately

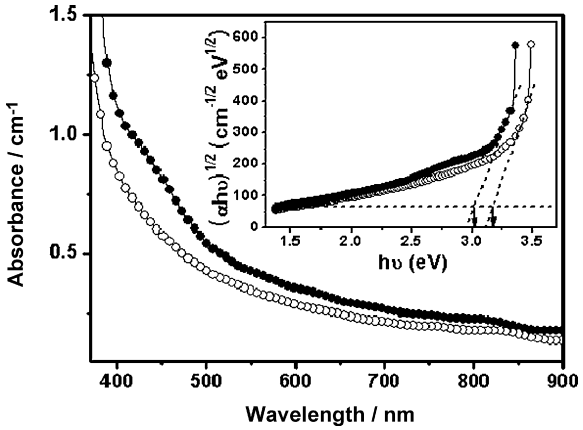

Fig. 3. UV–vis spectra of anatase and rutile TiO_2 film, measured using FTO glass as reference. Inset shows calculated band gaps of both films (open circles are anatase TiO_2 film; closed circles are rutile TiO_2 film).

3.17 eV and 3.01 eV, respectively. These are similar to previously reported values and confirm the growth of the pure anatase and the rutile TiO_2 film [27].

The electron diffusion coefficients and lifetimes as a function of J_{sc}, for the anatase and rutile TiO_2 electrodes are given in Fig. 4. In the case of the pure rutile TiO_2 electrode, a degraded rate of electron transport associated with a reduction in laser intensity is exhibited in relation to the non-parallel slope relative to the pure anatase TiO_2 electrode, which indicates the distribution of defect states in the proximity of the flat-band potential (V_{FB}). That is, the distribution of defect states is deviated in both electrodes, resulting from the intrinsic properties of anatase/rutile materials and the different morphological structure in the growth process [28]. Compared with the pure anatase TiO_2 electrode, the decreased rate of electron transport in the pure rutile TiO_2 electrode is attributed to the influence of morphology, such as a rougher columnar structure composed of small grains, an increased surface area, frequent trapping/detrapping along the grain boundaries and the original rutile property of larger electron effective mass and, hence, lower mobility [29].

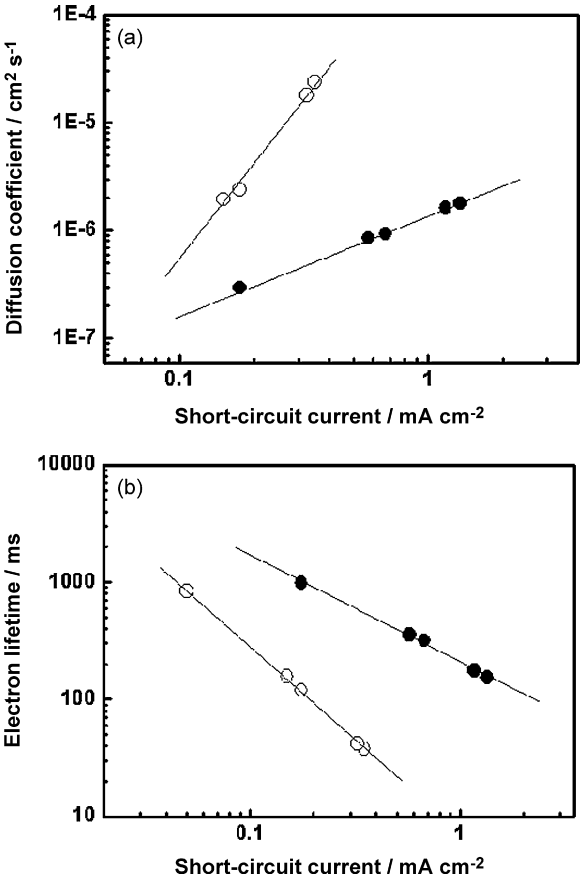

Fig. 4. (a) D and (b) τ in DSSCs, based on anatase and rutile TiO_2 electrodes (open circles are anatase TiO_2 film; closed circles are rutile TiO_2 film).

The above seems to be a counterproductive result, in spite of the high density (4.25 g cm^{-3}) of the rutile TiO_2 phase, and is due to the more compact structure (lattice constant; a = 0.45937 nm and c = 0.29587 nm) and good conditions for electron transport on account of the growth of a specific direction in the (1 1 0) plane. Park et al. [22] reported similar results by applying chemically synthesized anatase and rutile TiO_2 nanoparticles in DSSCs. It was concluded that the anatase TiO_2 film exhibited enhanced conversion efficiency, due to both the rapid rate of electron transport and the large surface area of the highly inter-connected network. By contrast, the rutile TiO_2 film exhibited a degraded performance of approximately 30%, because of the lower adsorption of dye molecules and the slower electron transport.

Based on these results, it can be concluded that modification of surface morphology using the RF sputtering method, which is a type of physical vapour deposition, can play an essential role in enhancing conversion efficiency, even though the intrinsic property of rutile TiO_2 as a photoanode layer in DSSC has a lesser effect from the perspective of conversion efficiency. Moreover, poor electron diffusion also results in a significant increase in electron lifetime, as shown in Fig. 4(b). Since the lifetime, measured with the SLIM-PCV, indicates a property of an individual electron, it is different from the overall photovoltaic property (*i.e.* V_{oc}) explained above.

In summary, pure anatase and rutile TiO_2 films have been deposited on a rugged FTO substrate, using the RF magnetron sputtering technique in which the substrate temperature is increased from 299 K to 623 K. Moreover, their application in DSSCs is achieved and yields an enhanced conversion efficiency in the rutile TiO_2 film (2.4%), compared with that of the anatase TiO_2 film (1.78%). The enhancement of the photovoltaic performance is attributed to an improved light-harvesting efficiency from an enlarged surface area that results from the extremely small size of the grains and rough surface morphology in a specific direction in the (1 1 0) plane, compared with the anatase TiO_2 film. Surface morphological properties and intrinsic material properties are considered to be factors that significantly contribute to enhancement of the efficiency of a DSSC, despite a trade-off in terms of the capacity for electron transport.

4. Conclusions

The growth and morphological control of a pure rutile TiO_2 film using the RF-magnetron sputtering method enhances the performance of DSSCs, compared with a pure anatase TiO_2 film. It is concluded that the columnar-structured rutile TiO_2 film prepared by the RF-magnetron sputtering method can be successfully used as the interlayer between the TCO and the mesoporous TiO_2 layer to enhance the charge-collection efficiency of the DSSC.

Acknowledgements

This work was supported in part by KOSEF (Contract No. R01-2004-000-10143-0), and in part by the Research Center for Energy Conversion and Storage (Contract No. R11-2002-102-00000-0).

References

[1] B. O'Regan, M. Grätzel, Nature 353 (1991) 737.
[2] S.H. Kang, S.-H. Choi, M.-S. Kang, J.-Y. Kim, H.-S. Kim, T. Hyeon, Y.-E. Sung, Adv. Mater. 20 (2008) 54.
[3] M. Law, L. Greene, J. Jonhson, R. Saykally, P. Yang, Nat. Mater. 4 (2005) 455.
[4] L. Greene, M. Law, J. Goldberger, F. Kim, J. Johnson, P. Yang, Angew. Chem. Int. Ed. 42 (2003) 3031.
[5] N.-G. Park, M.G. Kang, K.M. Kim, K.S. Ryu, S.H. Chang, A.J. Frank, Langmuir 20 (2004) 4246.
[6] A.N.M. Green, E. Palomares, S.A. Haque, J.M. Kroon, J.R. Durrant, J. Phys. Chem. B 109 (2005) 12525.
[7] T. Ma, M. Akiyama, E. Abe, I. Imai, Nano Lett. 5 (2005) 2543.
[8] K. Shankar, K.C. Tep, G.K. Mor, C.A. Grimes, J. Phys. D: Appl. Phys. 39 (2006) 2361.
[9] S.H. Kang, J.-Y. Kim, H.S. Kim, Y.-E. Sung, J. Phys. Chem. C 111 (2007) 9614.
[10] H.S. Jung, J.-K. Lee, M. Nastasi, Langmuir 21 (2005) 10332.
[11] K. Zhu, N.R. Neale, A. Miedaner, A.J. Frank, Nano Lett. 7 (2007) 69.
[12] K.-S. Ahn, M.-S. Kang, J.-W. Lee, Y.S. Kang, J. Appl. Phys. 101 (2007) 084312.
[13] L. Kavan, M. Grätzel, Electrochim. Acta 40 (1995) 643.
[14] S.H. Kang, J.-Y. Kim, Y. Kim, Y.-E. Sung, J. Photochem. Photobiol. A: Chem. 186 (2007) 234.
[15] S. Ito, P. Liska, P. Comte, M. Grätzel, Chem. Commun. (2005) 4351.
[16] J. Xia, N. Masaki, K. Jiang, S. Yanagida, J. Phys. Chem. B 110 (2006) 25222.
[17] S. Takeda, S. Suzuki, H. Odaka, H. Hosono, Thin Solid Films 392 (2001) 338.
[18] T.M. Wang, S.K. Zheng, W.C. Hao, C. Wang, Surf. Coat. Technol. 155 (2002) 141.
[19] S. Nakade, T. Kanzaki, Y. Wada, S. Yanagida, Langmuir 21 (2005) 10803.
[20] S. Nakade, T. Kanzaki, S. Kambe, Y. Wada, S. Yanagida, Langmuir 21 (2005) 11414.
[21] M. Pal, T. Sasaki, N. Koshizaki, Scripta Mater. 44 (2001) 1817.
[22] N.-G. Park, J. van de Lagemaat, A.J. Frank, J. Phys. Chem. B 104 (2000) 8989.
[23] W. Shindo, T. Ohmi, J. Appl. Phys. 79 (1996) 2347.
[24] H. Zhang, J.F. Bandfield, J. Mater. Chem. 8 (1998) 2073.
[25] J. Bisquert, A. Zaban, P. Salvador, J. Phys. Chem. B 106 (2002) 8774.
[26] K. Okimura, Surf. Coat. Technol. 135 (2001) 286.
[27] H. Poelman, H. Tomaszewski, D. Poelman, D. Depla, R. De Gryse, Surf. Interface Anal. 36 (2004) 1167.
[28] J. Nelson, Phys. Rev. B 59 (1999) 15374.
[29] S. Banerjee, J. Gopal, P. Muraleedharan, A.K. Tyagi, B. Raj, Curr. Sci. 90 (2006) 1378.